Taylor & Francis
Taylor & Francis Group

Phase Transitions

A Multinational Journal

ISSN: 0141-1594 (Print) 1029-0338 (Online) Journal homepage: https://www.tandfonline.com/loi/gpht20

Phase (*x*, *T*) and (*p*, *T*) diagrams of TlIn(S1−xSex)2 polycrystal in the compositional range 0≤x≤0.15

P. P. Guranich, R. R. Rosul, O. O. Gomonnai, V. M. Rubish, A. V. Gomonnai, A. G. Slivka & P. Huranych

To cite this article: P. P. Guranich, R. R. Rosul, O. O. Gomonnai, V. M. Rubish, A. V. Gomonnai, A. G. Slivka & P. Huranych (2019): Phase (*x*, *T*) and (*p*, *T*) diagrams of TlIn(S1−xSex)2 polycrystal in the compositional range 0≤x≤0.15, Phase Transitions, DOI: 10.1080/01411594.2019.1597097

To link to this article: https://doi.org/10.1080/01411594.2019.1597097

Published online: 28 Mar 2019.

PHASE TRANSITIONS
https://doi.org/10.1080/01411594.2019.1597097

Taylor & Francis
Taylor & Francis Group

Phase (x, T) and (p, T) diagrams of $TlIn(S_{1-x}Se_x)_2$ polycrystal in the compositional range $0 \leq x \leq 0.15$

P. P. Guranich[a], R. R. Rosul[a], O. O. Gomonnai[a], V. M. Rubish[b], A. V. Gomonnai[c], A. G. Slivka[a] and P. Huranych[a]

[a]Department of Optics, Uzhhorod National University, Uzhhorod, Ukraine; [b]Uzhhorod Scientific and Technological Centre for Materials of Optical Information Carriers, Institute for Information Recording, NAS of Ukraine, Uzhhorod, Ukraine; [c]Institute of Electron Physics, NAS of Ukraine, Uzhhorod, Ukraine

ABSTRACT

Temperature and pressure dependences of dielectric characteristics of $TlIn(S_{1-x}Se_x)_2$ polycrystals for $0 \leq x \leq 0.15$ are studied. Their phase (x, T) and (p, T) diagrams are built. With increasing Se content a broadening of the temperature interval of existence of the incommensurate phase is observed. Pressure coefficients of phase transition temperature shift are determined. A complex polycritical region in the pressure range 550–600 MPa is found.

ARTICLE HISTORY
Received 18 November 2018
Accepted 10 March 2019

KEYWORDS
Ferroelectrics; phase transition; dielectric permittivity; pressure; phase diagram

1. Introduction

A considerable interest towards $TlInS_2$-type crystals is related to the fact these crystals being ferroelectric semiconductors with a quasitwodimensional structure where a series of phase transformations occurs: paraelectric → incommensurate → ferroelectric phases [1–8]. A continuous row of $TlIn(S_{1-x}Se_x)_2$ solid solutions is known to be formed from $TlInS_2$ at S → Se substitution within $x \leq 0.7$ [9].

The present paper is devoted to the studies of dielectric properties in the vicinity of the phase transitions (PT) of $TlIn(S_{1-x}Se_x)_2$ polycrystals with Se content up to $x = 0.15$ aimed at the construction of (x, T) and (p, T) phase diagrams. Note that temperature and pressure dependences of dielectric permittivity ε of $TlInS_2$ crystal were studied in detail in a series of papers [4–8] while phase transitions in $TlIn(S_{1-x}Se_x)_2$ were investigated in Refs. [10, 11]. Based on the studies of $\varepsilon(T)$ in $TlIn(S_{1-x}Se_x)_2$ single crystals it was shown that isovalent substitution of S by Se results in the PT temperature decrease and the temperature interval of the incommensurate phase shrinks and at $x = 0.05$ in the (x, T) phase diagram a Lifshitz-type polycritical point exists [10]. Note that in our earlier paper [12] where the dielectric studies of $TlIn(S_{1-x}Se_x)_2$ polycrystals with Se content up to $x = 0.03$ were presented, contrary to the data of other authors [10, 11], we found no essential change of the incommensurate phase temperature interval at atmospheric pressure. Therefore, studies of the concentrations up to $x = 0.15$ are interesting at atmospheric pressure. Moreover, there are no studies performed of influence of isomorphic substitution S to Se on the regions of existence of high-pressure phases, that were found in $TlInS_2$ [13]. $TlInS_2$ crystal possess unique high anisotropy of physical properties [14, 15], therefore it is interesting to compare properties of mono- and polycrystals of $TlIn(S_{1-x}Se_x)_2$ solid solutions.

CONTACT P. P. Guranich pguranich@gmail.com

2. Experimental

$TlIn(S_{1-x}Se_x)_2$ polycrystals under investigation were obtained from the melt of a stoichiometric mixture of the initial $TlInS_2$ and $TlInSe_2$ components. For the characterisation of the $TlIn(S_{1-x}Se_x)_2$ polycrystals, X-ray diffraction (XRD) studies were carried out at room temperature using a conventional Bragg–Brentano technique with a DRON-4 diffractometer and Cu Ka radiation. Scanning electron microscopy (SEM) studies combined with energy-dispersive X-ray spectroscopy (EDX) were performed using a SEM JEOL 7000F microscope. Raman measurements were performed at room temperature on a LOMO DFS-24 double grating monochromator with a FEU-136 phototube and a photon counting system, the excitation being provided by a He–Ne laser (632.8 nm) and Ar^+ laser ($\lambda = 514.5$ nm). The instrumental width did not exceed 1 cm^{-1}. Dielectric permittivity studies of $4 \times 4 \times 2$ mm^3 samples were carried out at the frequency of 1 MHz using an automated setup with an AC bridge with temperature variation rate of 0.01–0.02 K/s. Contacts were made of silver paste. The sample temperature was measured by a copper-constantane thermocouple. Pressure studies were performed in the hydrostatic pressure range up to 750 MPa. The pressure was measured with the accuracy of 1 MPa. A high-pressure chamber with petrol being used as the working liquid.

3. Results and discussion

In order to check the chemical composition and quality of the samples their local elemental analysis by energy-dispersive X-ray fluorescence spectroscopy with SEM surface imaging was performed as well as Raman scattering and XRD studies.

X-ray diffraction patterns of the $TlIn(S_{1-x}Se_x)_2$ samples (a typical one is shown in Figure 1) reveal the main peaks whose positions are in good agreement with the data for the C_{2h}^6 space group (monoclinic structure). Note that in most cases such structure exists at room temperature and atmospheric pressure. With partial S→Se substitution in the polycrystals their XRD data exhibit a slight gradual shift of the $2\theta = (23.91 \pm 0.04)^\circ$ diffraction peak, i. e. with selenium content increase in the solid solutions a slight (up to 1% for $x = 0.07$) increase of the lattice parameter is observed.

A typical surface SEM image and the corresponding EDX spectrum for $TlIn(S_{1-x}Se_x)_2$ polycrystals are shown in Figure 2. Mass and atomic component ratios for the $TlIn(S_{1-x}Se_x)_2$ materials under investigation, estimated from the EDX data are listed in Table 1. Numerical evaluation of the content of thallium, indium, sulfur and selenium content correlates with the ratios expected from the

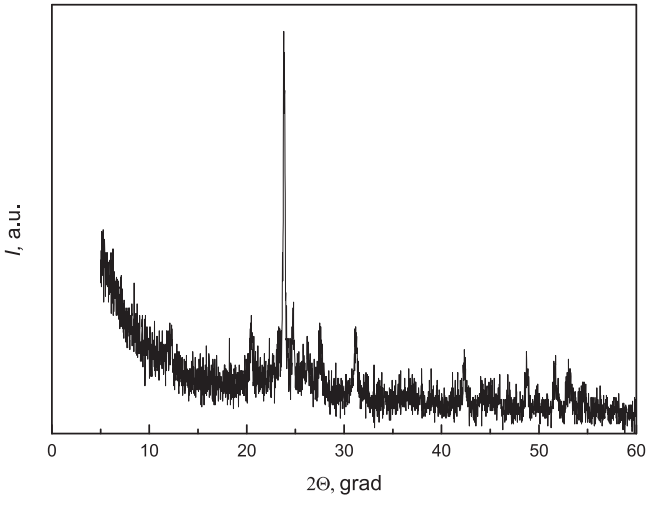

Figure 1. X-ray diffraction pattern of polycrystalline $TlIn(S_{0.96}Se_{0.04})_2$.

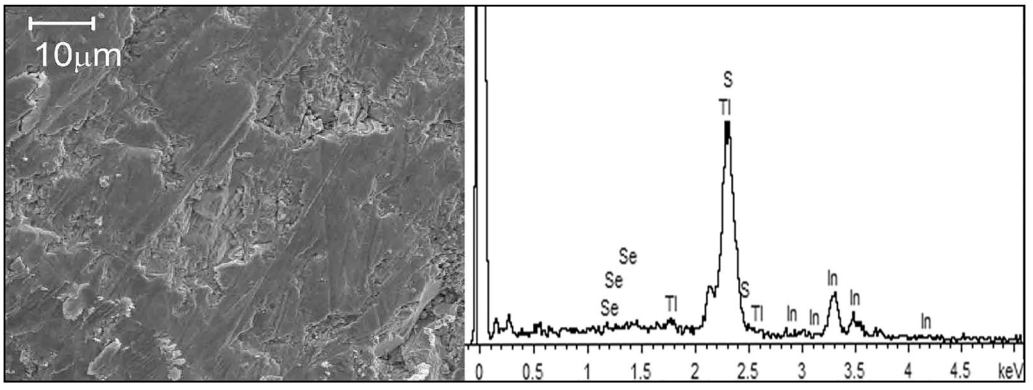

Figure 2. SEM pattern and EDX spectrum of the $TlIn(S_{0.96}Se_{0.04})_2$ polycrystals sample.

Table 1. Mass and atomic elemental content of materials under investigation based on EDX studies.

Compaund	Element	Weight %	Atomic %
$TlInS_2$	S	18.81	52.08
	In	37.33	28.86
	Tl	43.86	19.05
$TlIn(S_{0.99}Se_{0.01})_2$	S	15.77	46.95
	Se	0.48	0.58
	In	36,63	30.46
	Tl	47.12	22.01
$TlIn(S_{0.98}Se_{0.02})_2$	S	18.49	51.50
	Se	0.72	0.82
	In	36,29	28.23
	Tl	44.50	19.45
$TlIn(S_{0.96}Se_{0.04})_2$	S	15.03	45.29
	Se	1.09	1.34
	In	37.23	31.33
	Tl	46.64	22.05
$TlIn(S_{0.93}Se_{0.07})_2$	S	18.77	50.08
	Se	2.92	3.17
	In	42.83	31.91
	Tl	35.47	14.85

chemical formulae. However, slight deviations of thallium and indium content should be mentioned, namely an overestimation of In and underestimation of Tl concentration in our EDX studies.

Raman spectra of the $TlIn(S_{1-x}Se_x)_2$ polycrystals under investigation are shown in Figure 3. Note that the Raman spectra measured here are in agreement with the earlier data ([16, 17] and references therein).

It is known, e.g. [16, 17], that higher-frequency Raman bands of $TlInS_2$ correspond to 'intramolecular' vibrations of comparatively rigid tetrahedral In_4S_{10} structural groups bound by ion-covalent bonds with Tl atoms located in the voids between them. Meanwhile, lower-frequency bands correspond to translational vibrations governed by weaker interactions of van-der-Waals type for the bonds between the In_4S_{10} tetrahedra and ionic forces binding Tl^+ to InS_2^- ions.

Substitution of S with Se in the compositional range under investigation practically does not affect the lower-frequency part of the Raman spectra of $TlIn(S_{1-x}Se_x)_2$ polycrystals. Simultaneously, in the higher-frequency range even at low selenium concentration new bands appear in the range 180–210 cm^{-1} which can be, similarly to the case of single crystals [17], related to the vibrations of S and Se atoms in 'mixed' $In_4S_{10-y}Se$ tetrahedra. Note that the isovalent substitution of sulfur by selenium results in a slight frequency decrease of high-energy bands at 280, 291, and 345 cm^{-1} corresponding

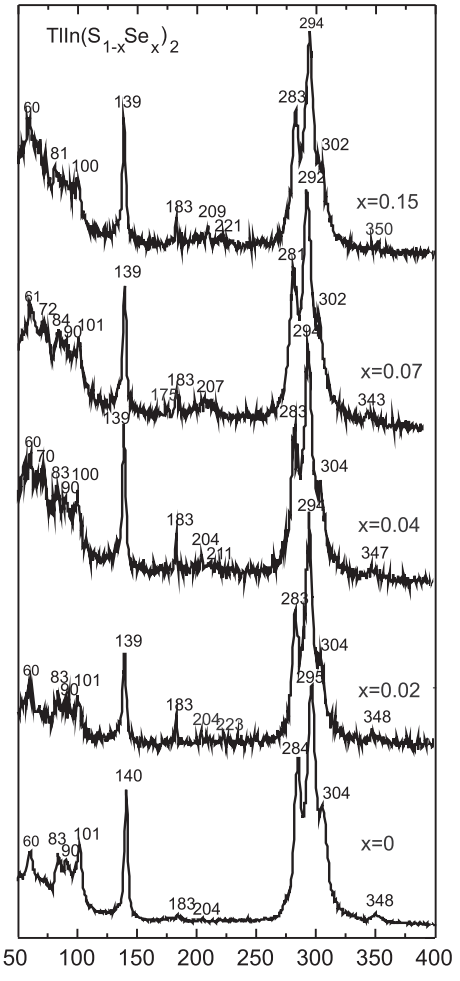

Figure 3. Raman spectra of the $TlIn(S_{1-x}Se_x)_2$ polycrystals.

to the 'intramolecular' vibrations of In_4S_{10} tetrahedra as well as the decrease of frequency of the band at 140 cm^{-1} for $TlInS_2$ by several reciprocal centimetres what in general is in agreement with the Raman data for $TlIn(S_{1-x}Se_x)_2$ single crystals [17].

As follows from the XRD and EDX data as well as the Raman spectra of $TlIn(S_{1-x}Se_x)_2$ polycrystals, the sulfur and selenium concentration ratios correlate well with the chalcogen content in the initial mixture and the polycrystalline samples under study are isostructural and correspond to the chemical composition.

In order to identify the anomalies of dielectric permittivity in the phase transition range for $TlIn(S_{1-x}Se_x)_2$ polycrystals, the dielectric characteristics of single crystalline and polycrystalline $TlInS_2$ were compared.

Figure 4 shows the temperature dependences of the dielectric permittivity ε and dielectric loss tangent tanδ for single crystalline and polycrystalline $TlInS_2$.

As can be seen from Figure 4, for single crystalline $TlInS_2$ in the temperature dependences of the dielectric permittivity ε_a (along the layers) and ε_c (normally to the layers) a number of anomalies is revealed, corresponding to the phase transitions at the temperatures $T_i = 214$ K, $T_{i2} = 206$ K, $T_{c1} = 202$ K, $T_{c2} = 198$ K, and $T_c = 193$ K what is in agreement with the known data [3–7]. Note that the mechanisms of these transitions are considered in Refs. [3] and [7]. The anomaly at T_i

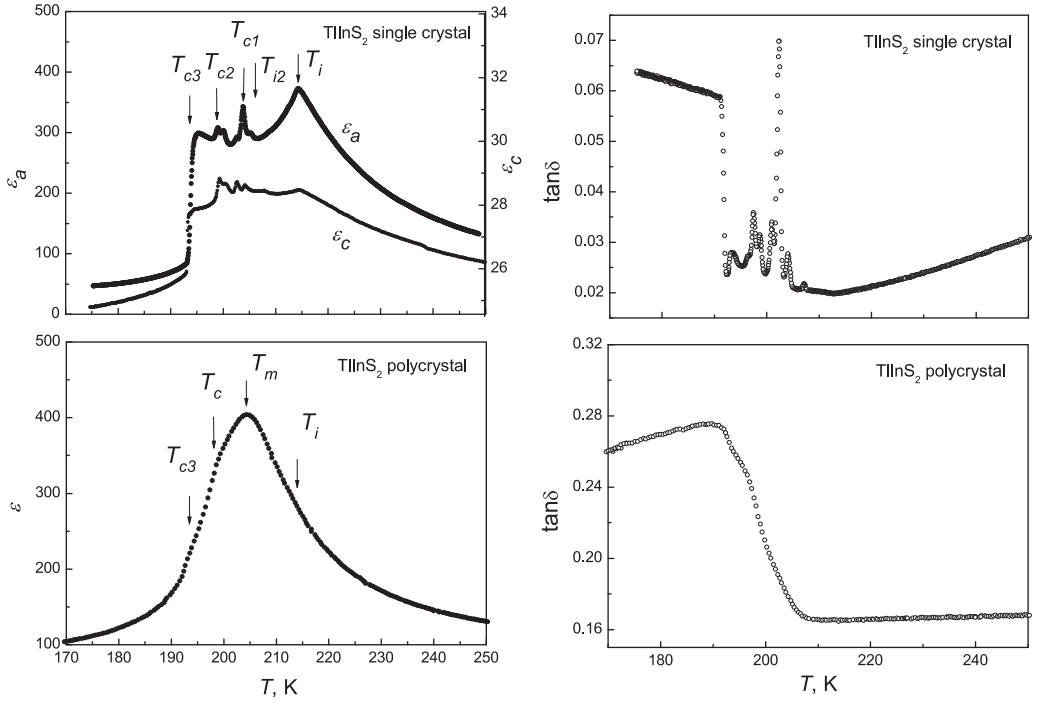

Figure 4. Temperature dependences of the dielectric permittivity ε and dielectric loss tangent tanδ for single crystalline and polycrystalline $TlInS_2$.

corresponds to the transition from paraelectric phase to incommensurate phase 1, the one at T_{i2} corresponds to the transition from incommensurate phase 1 to incommensurate phase 2, the one at T_{c1} corresponds to the transition from incommensurate phase 1 to ferroelectric phase 1, the one at T_{c2} corresponds to the transition from incommensurate phase 2 to ferroelectric phase 2, and that at T_{c3} corresponds to the transition to proper ferroelectric phase. Thus, the temperature range of existence of the incommensurate structure in these crystals is between T_i and T_{c2}. Note that based on the NMR studies [18] it was shown that the incommensurate phase in the simplest single-layer polytype with c = 15 Å corresponds to the temperature range of 192–205 K while the anomalies at 201 K and 216 K are explained by the presence of other polytypes.

As can be seen from Figure 4, the anomalies of dielectric permittivity in polycrystalline $TlInS_2$ are observed at the same temperatures as for $TlInS_2$ single crystal, however in the polycrystal these anomalies are strongly smeared. The dielectric permittivity achieves its maximal value at the temperature $T = T_m$ which is close to T_{i2} and T_{c1}. Evidently, this maximum is the result of superimposement of the anomalies atT_{i2} and T_{c1} located close to each other, hence we can assign T_m to the incommensurate 1 – incommensurate 2 phase transition. The anomaly at T_i corresponds to the transition from the paraelectric phase to the incommensurate phase 1 and the one at T_c corresponds to the transition from the incommensurate phase 2 to the ferroelectric phase 2 (T_c coincides with T_{c2} for the single crystal). Hence, the interval of existence of the incommensurate structure in the polycrystals corresponds to the temperature range between T_i and T_c. Note that smearing of $\varepsilon(T)$ anomalies is characteristic not only for polycrystalline $TlIn(S_{1-x}Se_x)_2$ samples, but also for the single crystals where it was observed [10, 11] and explained by non-equivalence of the substitutive S→Se sites in $In_4S(Se)_6$ complexes in different parts of the crystal.

Figure 5 illustrates the temperature dependences of dielectric permittivity ε for $TlIn(S_{1-x}Se_x)_2$ polycrystals with x = 0, 0.01, 0.03, 0.05, 0.07, and 0.15. These dependences, similarly to the case of polycrystalline $TlInS_2$, reveal an anomaly of $\varepsilon(T)$ in the form of a maximum at the temperature

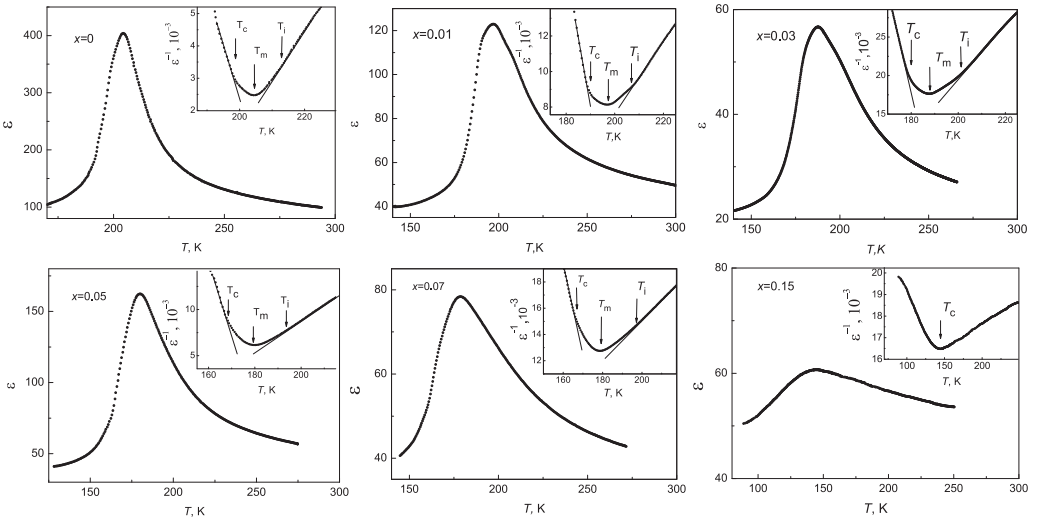

Figure 5. Temperature dependences of dielectric permittivity ε for $TlIn(S_{1-x}Se_x)_2$ polycrystals at atmospheric pressure. The inserts show the temperature dependences of ε^{-1}.

T_m accompanied by an additional anomaly at higher temperatures in the form of an inflection at $T = T_i$ and an anomaly at lower temperatures in the form of a low-temperature shoulder at $T = T_c$. For example, for $TlIn(S_{0.99}Se_{0.01})_2$ the temperatures of the anomalies are the following: $T_c = 189$ K, $T_m = 197$ K, $T_i = 207$ K. The inserts to Figure 5 also show the temperature dependences of ε^{-1} where the anomalies at T_c and T_i are revealed more distinctly due to the deviation of the $\varepsilon(T)$ dependence from linear law.

The increase of Se concentration in $TlIn(S_{1-x}Se_x)_2$ polycrystals results, in general, in a decrease of the dielectric permittivity value and a shift of the anomalies towards lower temperatures. The spread of the maximal values of $\varepsilon(x)$ is evidently related to the fact that the polycrystalline samples under investigation were not completely isotropic. Variation of temperatures T_i, T_m, and T_c at the isovalent substitution of sulfur by selenium determined from the temperature dependences of the dielectric permittivity for $TlIn(S_{1-x}Se_x)_2$ polycrystals is shown in Figure 6.

The compositional dependences of $T_i(x), T_m(x)$, and $T_c(x)$ are well described by the following expressions: $T_i = (214.3 - 780.5x + 7160x^2)$ K, $T_m = (203.4 - 659.1x + 3464x^2)$ K, $T_c = (196.2 - 650.5x + 2072x^2)$ K. Note that the interval between T_i and T_c increases with Se

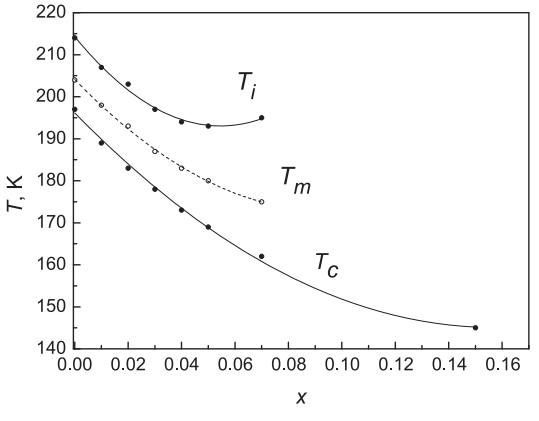

Figure 6. (x, T) phase diagram of $TlIn(S_{1-x}Se_x)_2$ polycrystals.

content. The compositional behaviour of $T_i(x)$ is nonlinear and at $x \approx 0.05$ the sign of the dT_i/dx coefficient is changed. Such compositional behaviour of the paraelectric-to-incommensurate PT can be explained by the effect of the electron subsystem on the incommensurate PT [19]. Note that for the polycrystals the compositional behaviour of T_i and T_m at $x < 0.05$ is in agreement with the data for $TlIn(S_{1-x}Se_x)_2$ single crystals [10, 11]. However, contrary to Ref. [10], we observe a reverse bending of the compositional dependences of the PT temperatures.

For $TlIn(S_{1-x}Se_x)_2$ polycrystals pressure studies of dielectric permittivity were performed. Temperature dependences of the real and imaginary parts of the dielectric permittivity of $TlIn(S_{1-x}Se_x)_2$ polycrystals at various hydrostatic pressure values measured in the heating mode are shown in Figure 7. With pressure increase up to 550 MPa, the anomalies of the dielectric permittivity shift linearly towards higher temperatures. The maximal values of the dielectric permittivity are observed to decrease and the temperature interval of existence of the incommensurate phase broadens. Due to the pressure-related broadening of the temperature interval of existence of the incommensurate phase with pressure increase to 550 MPa, the anomalies of the dielectric permittivity at T_i, T_m, and T_c are revealed more distinctly (see Figure 7). The pressure coefficients of the PT temperatures are listed in Table 2.

At pressures $p > 550$ MPa, qualitative changes in the $\varepsilon'(T)$ dependence occur, revealed as a decrease of the maximal permittivity values and a transformation of the anomalies. Similarly to the case of $TlInS_2$ single crystal [8], the changes in the $\varepsilon'(T)$ dependences result from polycritical phenomena in the (p,T) phase diagram of the $TlIn(S_{1-x}Se_x)_2$ polycrystals shown in Figure 8. The region above the $T_i(p)$ transition line corresponds to the paraelectric phase while the region of existence of the incommensurate structure is restricted by $T_i(p)$ and $T_c(p)$ lines. The area below the $T_c(p)$ transition line corresponds to the ferroelectric phase. Dashed lines in the (p,T) diagrams corresponds to the transitions to high-pressure phases at T_1 and T_2. The $T_1(p)$ and $T_2(p)$ lines are first-order PT lines with a considerable (temperature and pressure) hysteresis. The detailed studies of the nature of these transitions and high pressure phases for $TlInS_2$ crystals were performed in Ref [13].

As can be seen from Figure 8, in the range of pressures 550–600 MPa the phase transition lines $T_i(p)$, $T_m(p)$ and $T_c(p)$ intersect with $T_1(p)$ and $T_2(p)$. The dielectric permittivity in the vicinity of the phase transitions at T_i, T_m, and T_c sharply decreases. Such behaviour of the dielectric permittivity is caused by the transitions to high-pressure phases [13] and requires additional studies to be explained. Phase transition lines $T_1(p)$ and $T_2(p)$ were additionally investigated by pressure studies

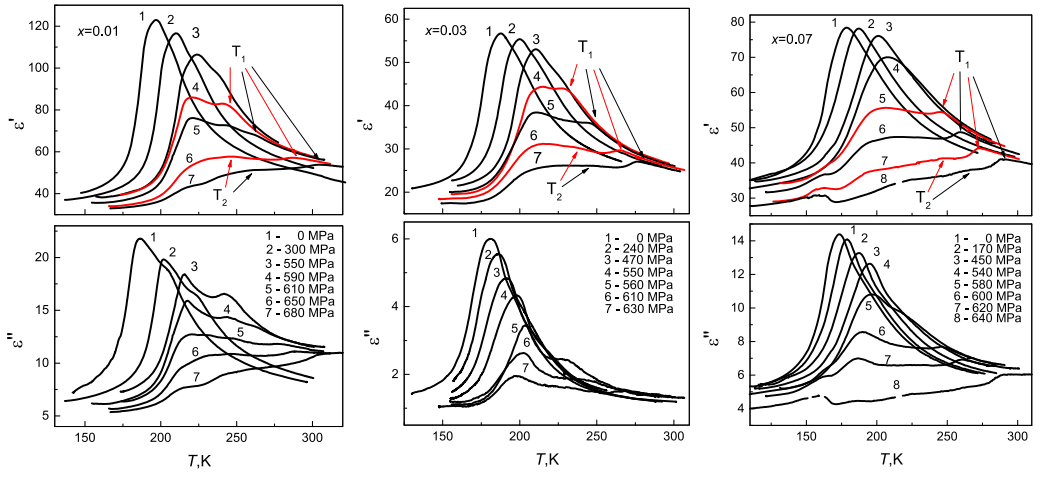

Figure 7. Temperature dependences of ε' and ε'' for $TlIn(S_{1-x}Se_x)_2$ polycrystals at various hydrostatic pressure values. The arrows show the anomalies of $\varepsilon'(T)$ at phase transitions to high-pressure phases at T_1 and T_2 corresponding to the T_1 and T_2 lines and the open circles in Figure 8.

Table 2. Pressure coefficients of the PT temperature shift for $TlIn(S_{1-x}Se_x)_2$ polycrystals.

x	0	0.01	0.02	0.03	0.04	0.05	0.07	0.15
dT_i/dp, K/GPa	56	55	56	56	57	56	59	–
dT_m/dp, K/GPa	46	47	50	49	51	53	55	–
dT_c/dp, K/GPa	44	42	44	44	46	48	50	53

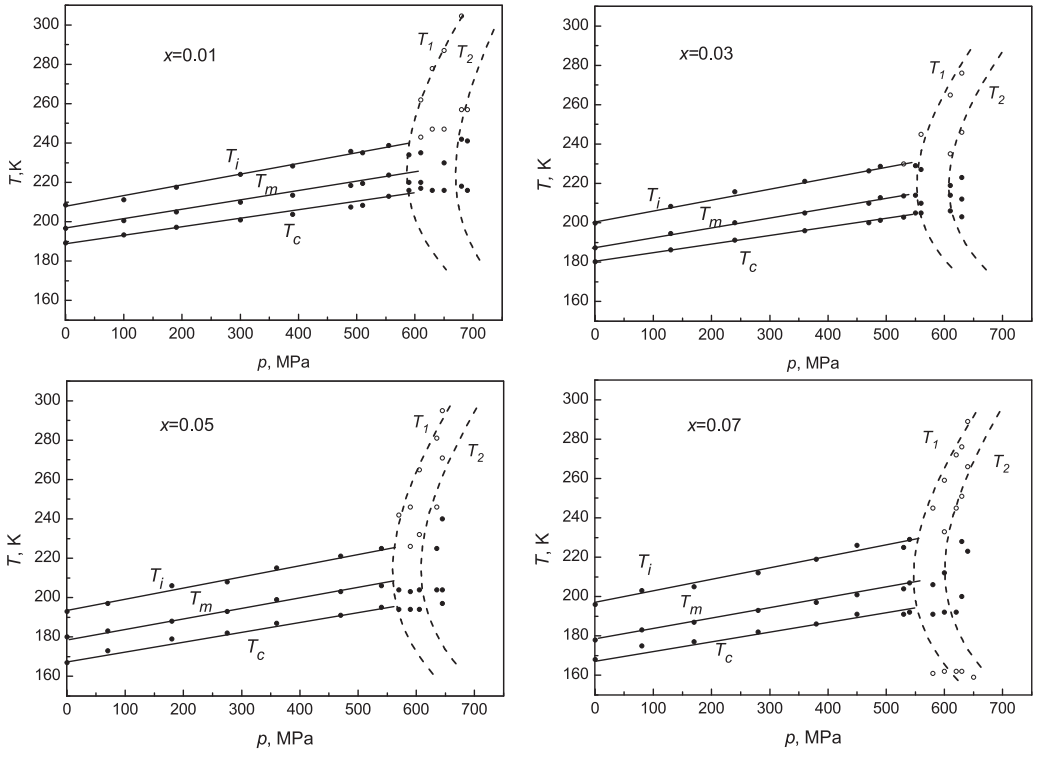

Figure 8. (p, T) phase diagram of $TlIn(S_{1-x}Se_x)_2$ polycrystals (heating mode).

of dielectric permittivity at fixed temperatures. At phase transitions pressures, that correspond T_1 and T_2 jump-like anomalies of ε are observed, similarly to monocrystal $TlInS_2$ [13].

The following features of the polycritical region common for the $TlIn(S_{1-x}Se_x)_2$ under investigation should be pointed out. First, the transition to the high-pressure phase occurs in two stages, i.e. two PTs with the formation of an intermediate phase take place successively with increasing pressure. Second, the transformation of anomalies of the dielectric permittivity with pressure occurs gradually and the 'traces' of the PT lines are detected in the high-pressure phase at T_i, T_m, and T_c are detected, vanishing with the pressure increase. This can be explained by the fact that in these materials the features are related to the weak interaction of several order parameters and/or the coexistence of crystal domains with different phases.

4. Conclusions

The studies performed show that in $TlIn(S_{1-x}Se_x)_2$ polycrystals with increasing Se content the anomalies of dielectric properties corresponding to the incommensurate phase transitions nonlinearly shift towards lower temperatures. A broadening of the temperature interval of existence of

the incommensurate phase is observed and the Lifshitz point which is, according to Ref. [10] for single crystalline $TlIn(S_{1-x}Se_x)_2$ expected at $x \approx 0.05$, is not revealed for the polycrystals.

Based on the investigation of the temperature and pressure dependences of dielectric properties of the $TlIn(S_{1-x}Se_x)_2$ polycrystals, their (x,T) and (p,T) phase diagrams were built. Pressure coeffcients of the phase transition temperature shift are determined.

Disclosure statement

No potential conflict of interest was reported by the authors.

References

[1] Kashida S, Kobayashi Y. X-ray study of the incommensurate phase of TlInS. J Phys Condens Matter. 1999;11:1027–1035.

[2] Panich AM. Electronic properties and phase transition in low-dimensional semiconductors. J Phys Condens Matter. 2008;20:293202-1–293202-42.

[3] Suleimanov RA, Seidov MYu, Salaev FM, et al. Model of sequential structural phase transitions in $TlInS_2$ layered crystal. Fiz Tverd Tela. 1993;35:348–354.

[4] Allakhverdiev KR, Turetken N, Salaev FM, et al. Succession of the low temperature phase transitions in $TlInS_2$ crystals. Solid State Commun. 1995;96:827–831.

[5] Salaev FM, Allakhverdiev KR, Mikailov FA. Dielectric properties and metastable states in ferroelectric $TlInS_2$ crystals. Ferroelectrics. 1992;131:163–167.

[6] Mikailov FA, Basaran E, Mammadov TG, et al. Dielectric susceptibility behaviour in the incommensurate phase of $TlInS_2$. Phys B. 2003;334:13–20.

[7] Mikailov FA, Basaran E, Senturk E. Improper and proper ferroelectric phase transitions in $TlInS_2$ layered crystal with incommensurate structure. J Phys Condens Matter. 2001;13:727–733.

[8] Gomonnai OO, Guranich PP, Rigan MY, et al. Effect of hydrostatic pressure on phase transitions in ferroelectric $TlInS_2$. High Press Res. 2008;28:615–619.

[9] Özkan H, Gasanly N, Çulfaz A. Effect of isomorphic atom substitution on lattice parameters of $TlBX_2$-type mixed crystals. Turk J Phys. 1996;20:800–804.

[10] Seyidov M-HYu, Suleymanov RA, Salehli F. Effect of the 'negative chemical' pressure on the temperatures of phase transitions in the $TlInS_2$ layered crystal. Phys Solid State. 2009;51:2513–2519.

[11] Seyidov M-HYu, Suleymanov RA, Salehli F. Origin of structural instability in $TlInS_{2(1-x)}Se_{2x}$ solid solutions. Phys Scr. 2011;84:015601.

[12] Rosul RR, Guranich PP, Gomonnai OO, et al. Dielectric properties of $TlIn(S_{1-x}Se_x)_2$ polycrystals near phase transitions. Semiconduct Phys Quantum Electron Optoelectron. 2012;15(1):35–37.

[13] Guranich PP, Rosul RR, Gomonnai OO, et al. Ferroelasticity of $TlInS_2$ crystal. Solid State Commun. 2014;184:21–24.

[14] Martynyuk-Lototska I, Trach I, Kokhan O, et al. Efficient acousto-optic crystal, $TlInS_2$: acoustic and elastic anisotropy. Appl Opt. 2017;56:3179–3184.

[15] Say A, Martynyuk-Lototska I, Adamenko D, et al. Thermal expansion anisotropy of β-$TlInS_2$ crystals in the course of phase transitions. Phase Transit. 2017;91(1):1–8.

[16] Yuksek NS, Gasanly NM, Aydinli A. Anharmonic line shift and linewidth of the Raman modes in $TlInS_2$ layered crystals. J Raman Spectrosc. 2004;35:55–60.

[17] Gomonnai AV, Petryshynets I, Azhniuk YuM, et al. Growth and characterisation of sulphur-rich $TlIn(S_{1-x}Se_x)_2$ single crystals. J Cryst Growth. 2013;367:35–41.

[18] Panich AM, Mogilyansky D, Sardarly RM. Phase transitions and incommensurability in the layered semiconductor $TlInS_2$ – an NMR study. J Phys Condens Matter. 2012;24:135901.

[19] Mamin RM. Effect of thermal filling of trapping centers on the stability of structural phases in semiconductors. JETP Lett. 1993;58(7):538–542.